Activation of Protein Kinase C-ζ in Pancreatic β-Cells In Vivo Improves Glucose Tolerance and Induces β-Cell Expansion via mTOR Activation

Silvia Velazquez-Garcia,[1] Shelley Valle,[1] Taylor C. Rosa,[1] Karen K. Takane,[1] Cem Demirci,[2] Juan C. Alvarez-Perez,[1] Jose M. Mellado-Gil,[1] Sara Ernst,[1] Donald K. Scott,[1] Rupangi C. Vasavada,[1] Laura C. Alonso,[1] and Adolfo Garcia-Ocaña[1]

OBJECTIVE—PKC-ζ activation is a key signaling event for growth factor–induced β-cell replication in vitro. However, the effect of direct PKC-ζ activation in the β-cell in vivo is unknown. In this study, we examined the effects of PKC-ζ activation in β-cell expansion and function in vivo in mice and the mechanisms associated with these effects.

RESEARCH DESIGN AND METHODS—We characterized glucose homeostasis and β-cell phenotype of transgenic (TG) mice with constitutive activation of PKC-ζ in the β-cell. We also analyzed the expression and regulation of signaling pathways, G1/S cell cycle molecules, and β-cell functional markers in TG and wild-type mouse islets.

RESULTS—TG mice displayed increased plasma insulin, improved glucose tolerance, and enhanced insulin secretion with concomitant upregulation of islet insulin and glucokinase expression. In addition, TG mice displayed increased β-cell proliferation, size, and mass compared with wild-type littermates. The increase in β-cell proliferation was associated with upregulation of cyclins D1, D2, D3, and A and downregulation of p21. Phosphorylation of D-cyclins, known to initiate their rapid degradation, was reduced in TG mouse islets. Phosphorylation/inactivation of GSK-3β and phosphorylation/activation of mTOR, critical regulators of D-cyclin expression and β-cell proliferation, were enhanced in TG mouse islets, without changes in Akt phosphorylation status. Rapamycin treatment in vivo eliminated the increases in β-cell proliferation, size, and mass; the upregulation of cyclins Ds and A in TG mice; and the improvement in glucose tolerance—identifying mTOR as a novel downstream mediator of PKC-ζ–induced β-cell replication and expansion in vivo.

CONCLUSIONS—PKC-ζ, through mTOR activation, modifies the expression pattern of β-cell cycle molecules leading to increased β-cell replication and mass with a concomitant enhancement in β-cell function. Approaches to enhance PKC-ζ activity may be of value as a therapeutic strategy for the treatment of diabetes. *Diabetes* 60:2546–2559, 2011

Diabetes appears when β-cell mass is insufficient to maintain normal glucose homeostasis. Therefore, deciphering the molecular mechanisms that induce β-cell expansion can be of great value for therapeutic approaches aimed at increasing β-cell mass in diabetes. Atypical protein kinase C (PKC)-ζ, a relatively novel downstream target of phosphatidylinositol (PI) 3-kinase–phosphoinositide-dependent kinase-1 (PDK-1) in β-cells, is critical for mitogenic signal transduction in a variety of cell types, including fibroblasts, glial cells, and oocytes (1,2). PKC-ζ is expressed in insulinoma cells, as well as in rodent and human islets, and it is phosphorylated/activated by growth factors and nutrients such as glucose and free fatty acids (3–8). Importantly, activation of PKC-ζ is required for growth factor–stimulated β-cell proliferation in vitro (3,4). Furthermore, PKC-ζ overexpression enhances insulin-like growth factor-1 and insulin- and serum-induced proliferation in insulinoma cells in vitro (9). Taken together, these results highlight PKC-ζ as a critical signaling target for growth factor–mediated β-cell proliferation in vitro. Indeed, constitutively active PKC-ζ (CA-PKC-ζ) increases β-cell proliferation in insulinoma and primary mouse and human islet cells in vitro (3,4). Although the intracellular targets of PKC-ζ that induce mitogenesis are being actively explored in many tissues and include the extracellular signal–regulated kinases (ERK)1/2 and -5, glycogen synthase kinase 3 (GSK-3), mammalian target of rapamycin (mTOR) and p70S6 kinase (p70S6K) (10–14), whether these targets are activated by PKC-ζ in β-cells is unknown.

Studies using a variety of PKC inhibitors have suggested that glucose-stimulated insulin secretion (GSIS) is in part dependent on atypical PKCs activation in rat islets (6). In addition, inhibition of glucose-mediated activation of PKC-ζ correlates with decreased sulphonylurea receptor 1 (SUR1), inward rectifier K$^+$ channel subunit (Kir6.2), and forkhead box A2 (Foxa2) expression and diminished GSIS (7). Interestingly, it has been suggested that PKC-ζ could be involved in glucose-mediated DNA-binding activity of pancreatic and duodenal homeobox 1 (Pdx-1) to the insulin gene in MIN6 cells (5). Taken together, these in vitro studies strongly suggest that PKC-ζ activation in β-cells could lead to increased β-cell function, proliferation, and mass and improved glucose homeostasis in vivo. However, this has never been explored.

To analyze the effects of PKC-ζ activation in the β-cell in vivo, we generated transgenic (TG) mice with CA-PKC-ζ expression in the β-cell by using the rat insulin-II promoter (RIP). TG mice show increased β-cell replication, size, and
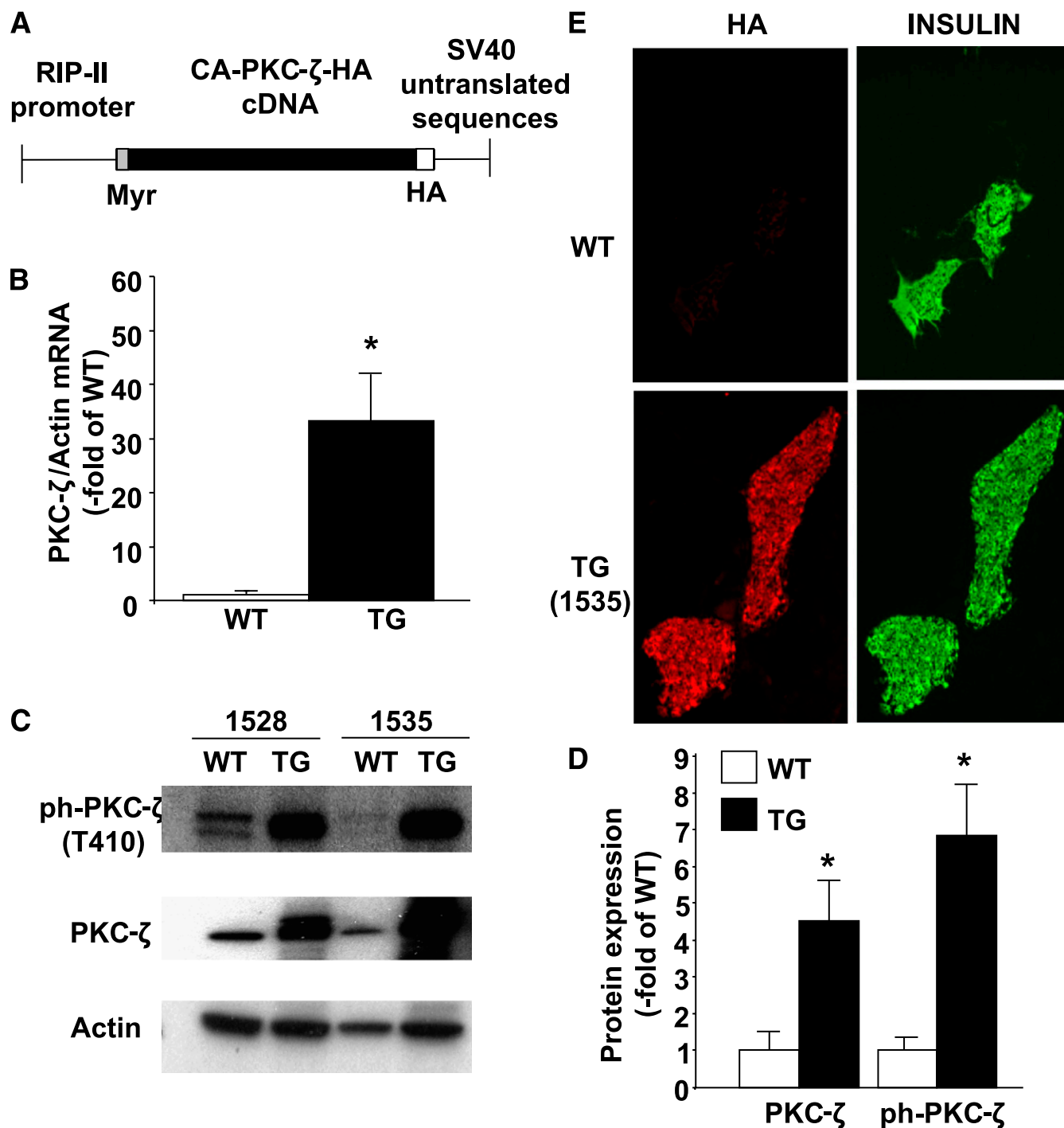
FIG. 1. Construction and expression of the transgene. *A*: Schematic illustration of the transgene construct. This construct contains a 650-bp segment of the promoter region of the rat insulin II gene (15) upstream of a myristoylated and constitutively activated form of PKC-ζ generated by the in-frame addition of the first nine amino acids of the p60 c-Src myristoylation sequence in the NH₂-terminal region of PKC-ζ. We added an HA tag at the COOH terminus of PKC-ζ for monitoring expression followed by SV-40 T-antigen 3′-untranslated region sequences containing transcription termination, polyadenylation, and splicing signals at the 3′ end of the transgene. *B*: Real-time PCR analysis of PKC-ζ gene expression in total islet RNA extracted from WT and TG mouse islets isolated at 10–14 weeks of age. Results are means ± SEM of WT (*n* = 5) and TG (*n* = 5) (lines 1535 and 1528) mice. *P < 0.05 vs. WT mice. *C*: Expression and phosphorylation of PKC-ζ was assessed by Western blot analysis of islet protein extracts from WT and TG mice at 10–14 weeks of age from both mouse lines (1528 and 1535). Actin was used as an internal control for loading. A representative immunoblot of three independent experiments is shown. Marked and similar increases in phospho–PKC-ζ-(T410) and total PKC-ζ were observed in both lines of TG mice. *D*: Quantification of the immunoblots in *D*. Results are means ± SEM of the ratio between phospho–PKC-ζ or PKC-ζ and actin in islets from WT (*n* = 5) and TG (*n* = 5) (lines 1535 and 1528) mice. *P < 0.05 vs. WT mice. *E*: Representative images of immunofluorescent staining for HA and insulin on pancreatic sections from WT and TG mice (line 1535) at 14 weeks of age. No HA staining was observed in islets from WT mice, but intense HA staining (left) colocalized with insulin staining (right) in TG mouse pancreas sections. (A high-quality color representation of this figure is available in the online issue.)
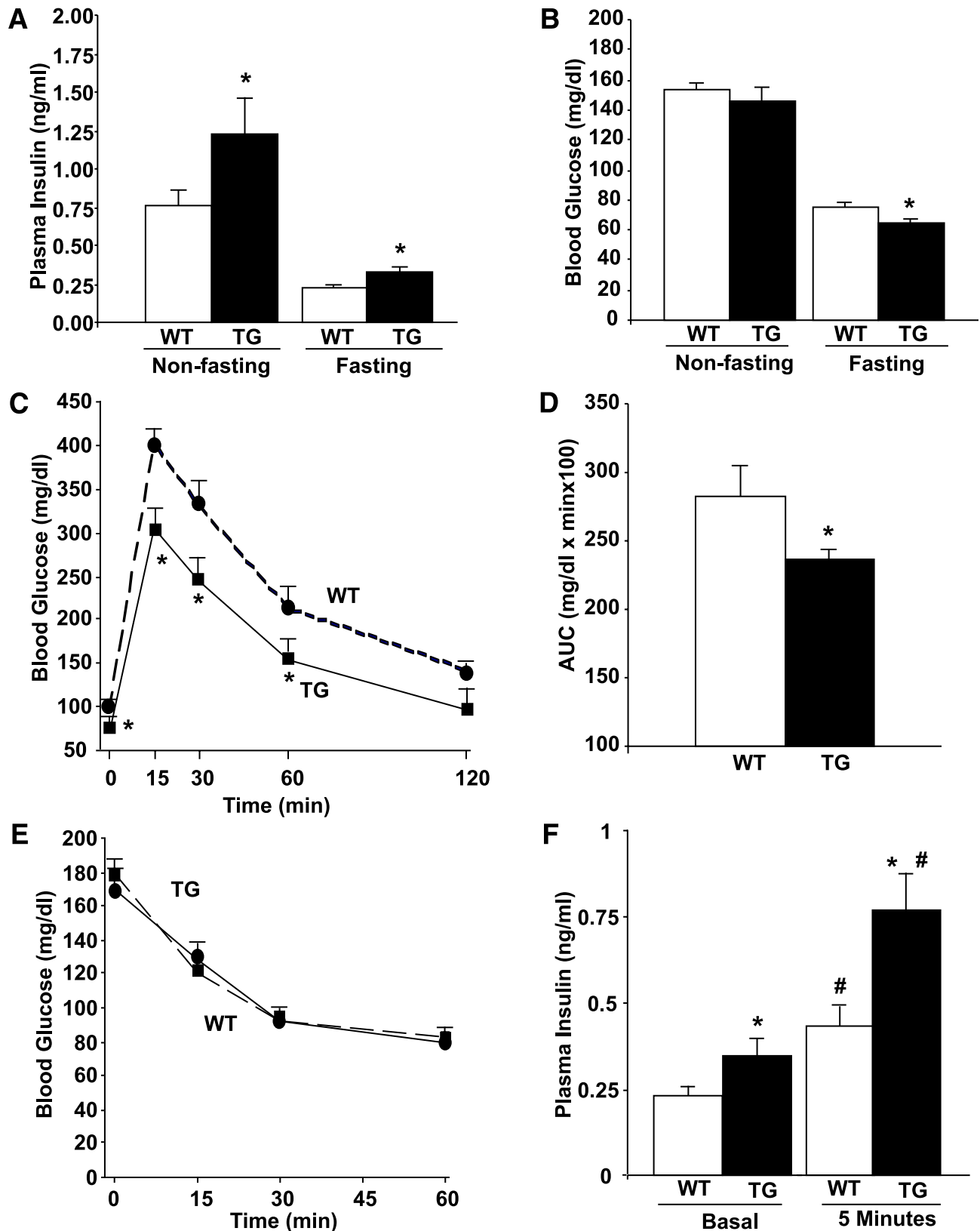
FIG. 2. Glucose homeostasis in RIP-CA-PKC-ζ mice. Plasma insulin (*A*) and blood glucose (*B*) levels in WT and TG mice at 10–14 weeks of age in nonfasting and fasting conditions. TG mice displayed hyperinsulinemia in both conditions and reduced blood glucose levels in fasting conditions. Results are means ± SEM of *n* = 15 WT and *n* = 10 TG mice. *P < 0.05 vs. WT mice in the same conditions. Intraperitoneal glucose tolerance test (*C*) and areas under the curve (AUCs) (*D*) calculated from these results in 12-week-old fasted WT (*n* = 15) and TG (*n* = 10) littermates injected intraperitoneally with 2 g glucose/kg body wt. Blood glucose levels were measured at the time points indicated. Results are means ± SEM. TG mice exhibited improved glucose tolerance, as revealed by significantly decreased blood glucose at the time points indicated and the AUC values. *P < 0.05 vs. WT. *E*: Insulin tolerance test performed in nonfasting 14-week-old WT (*n* = 15) and TG mice (*n* = 10). No significant differences were found in blood glucose levels before or after insulin administration in both types of mice. Values are means ± SEM. *F*: Plasma insulin in 12- to 14-week-old

mass concomitant with enhanced insulin secretion and improved glucose tolerance. These studies also uncover mTOR as a downstream key regulator of PKC-ζ effects in the β-cell. Our results clearly indicate that PKC-ζ activation could have therapeutic potential to expand β-cell mass and function for the treatment of diabetes.

RESEARCH DESIGN AND METHODS

Generation of RIP-CA-PKC-ζ TG mice. TG mice were generated as previously described (15). Briefly, the RIP-CA-PKC-ζ transgene was constructed with a 1.8-kb rat CA-PKC-ζ cDNA (generously provided by Dr. Alex Toker, Harvard Medical School, Boston, MA) downstream of the RIP-II (650 bp) and upstream of untranslated SV-40 sequences containing transcriptional termination, polyadenylation, and splicing signals. CA-PKC-ζ cDNA contains the NH_2-terminal c-src myristoylation signal along with a hemagglutinin (HA) tag at the COOH terminus for monitoring expression (Fig. 1A). The linearized construct (5.7 kb) was microinjected into C57BL6 mouse fertilized eggs (University of Pittsburgh Transgenic Mouse Facility), and potential founders were screened by tail DNA PCR using primers for exons 1 and 3 of PKC-ζ sequences (Supplementary Table 1) (16). For the rapamycin treatment studies, 0.5 mg/kg per day rapamycin (LC Laboratories, Woburn, MA) or the same volume of vehicle (0.4% DMSO) were injected intraperitoneally for 2 weeks.

All of the studies were performed on 10- to 14-week-old mice with the approval of, and in accordance with, guidelines established by the University of Pittsburgh Animal Care and Use Committee.

Islet isolation and mRNA expression analysis. Mouse islets were isolated as previously described (15). RNA (0.5–1 μg), isolated using the RNeasy micro kit (Qiagen, Valencia, CA), was reverse transcribed and the cDNA used as input for PCR using PerfeCTa SYBR Green FastMix (Quanta Biosciences, Gaithersburg, MD) and primers listed in Supplementary Table 1.

Western blot analysis. Protein extracts from tissues/cells were made in freshly prepared lysis buffer (2% SDS, 100 mmol/L Tris-HCl, pH 6.8, 1 mmol/L dithiothreitol, protease inhibitor cocktail [Roche, Mannheim, Germany]), 20 μg/mL phenylmethylsulfonyl fluoride, and 100 μmol/L Na_3VO_4). Cells/tissues were sonicated, supernatants separated by centrifugation, and protein concentrations measured using the MicroBCA assay (Pierce, Rockford, IL). Proteins (20–40 μg) per sample were added to loading buffer and analyzed using 7.5–12% SDS-PAGE. Proteins were transferred from the gels to Immobilon-P membrane (Millipore, Bedford, MA) using standard techniques. Blots were blocked in 5% nonfat dry milk and then incubated with primary antibodies (Supplementary Table 2). After several washes, blots were incubated with peroxidase-conjugated secondary antibodies and chemiluminescence was detected using an enhanced chemiluminescence system (Amersham Pharmacia Biotech, Piscataway, NJ) (3).

Immunohistochemistry, islet histomorphometry, and β-cell proliferation, size, and death. Paraffin-embedded pancreatic sections were immunostained for insulin and HA as previously described (17,18). β-Cell mass and islet size and number were measured in three insulin-stained pancreas sections per mouse using ImageJ (NIH, Bethesda, MD) (17). 5-bromo-2′-deoxyuridine (BrdU) incorporation in β-cells was measured in pancreas sections of mice injected intraperitoneally with BrdU (Amersham) and killed 6 h later. Sections were stained for insulin and BrdU (3), and 1,140 ± 64 β-cells were counted in blinded fashion per section. β-Cell death was determined in pancreas sections stained for insulin and the terminal deoxynucleotidyl transferase–mediated dUTP nick-end labeling (TUNEL) method (Promega, Madison, WI) (18), and 1,334 ± 107 β-cells/section were counted as described above. β-Cell size was measured in pancreatic sections stained for Glut-2 and insulin as previously described (19), and the size of at least 300 β-cells was quantified per section using ImageJ.

Body weight, food intake, and glucose homeostasis measurements. Body weight and food intake were quantified as reported (20). Blood was obtained from mice in the fasting state (16–18 h) or in the random-fed state by retroorbital bleeding as previously described (17). Blood glucose was determined using a glucometer (AlphaTRAK; Abbot, North Chicago, IL), and plasma insulin was measured by radioimmunoassay (RIA) (Linco, St. Louis, MO). Intraperitoneal glucose tolerance test (IPGTT) was performed in 16- to 18-h fasted mice injected intraperitoneally with 2 g D-glucose/kg body wt, and insulin tolerance test (ITT) was performed in random-fed mice injected intraperitoneally with 0.75 units bovine insulin/kg body wt (17). For measurement of insulin secretion in vivo, a different set of mice was fasted overnight and injected with

glucose as described above. Blood was collected before and 5 min after glucose injection, and plasma insulin was measured by RIA.

GSIS and islet insulin content. Insulin release from 10 islet equivalents (IEs) (1 IE = 125 μm diameter) was measured as previously described (17). After incubation in 5 or 22 mmol/L glucose, islets were washed, digested, and protein measured by the Bradford method. Results are expressed as the percentage of insulin secreted by wild-type (WT) islets at 5 mmol/L glucose (346 ± 46 pg insulin/μg protein/30 min). Islet insulin content was measured from isolated islets homogenized in acid/ethanol as previously described (17).

β-Cell proliferation in adenovirus-transduced INS-1 and mouse islet cells. Cells were transduced for 1 h with 100 multiplicity of infection (MOI) of adenovirus (Adv) containing the cDNA of CA-PKC-ζ (Adv-CA-PKC-ζ) or green fluorescent protein (Adv-GFP) as control, and INS-1 cell proliferation was assessed by [^{3}H]thymidine incorporation as previously described (3). β-Cell proliferation in primary mouse islet cell cultures was assessed in cells incubated in RPMI 1640 medium with 10% FBS, 5 mmol/L D-glucose, and BrdU (1:1,000 dilution) for 48 h. Insulin and BrdU staining was performed as previously described (3), and at least 2,000 β-cells/well were counted.

Statistical analysis. The data are presented as means ± SE. Statistical analysis was performed using unpaired two-tailed Student's t test or one-way ANOVA with Tukey post hoc test when several groups were analyzed. $P < 0.05$ was considered statistically significant.

RESULTS

Generation of RIP-CA-PKC-ζ TG mice. Five founder TG mice were identified: two failed to transmit the transgene to their progeny, and one died at 4 weeks of age. Thus, two lines (1,528 and 1,535) with germ-line integration of the transgene were obtained and maintained in a C57BL6 background. PKC-ζ mRNA and protein were upregulated in islets from TG mice compared with WT littermates (Fig. 1B–D). In addition, activation of PKC-ζ (Thr410 phosphorylation) was also highly and similarly increased in islets from both TG lines (Fig. 1C and D). On the other hand, phospho–PKC-ζ levels in brain protein extracts from TG and WT mice were not significantly different by immunoblot (phospho–PKC-ζ–to–tubulin ratio in WT, 1.0 ± 0.20, $n = 3$; TG, 1.2 ± 0.25, $n = 3$; $P = 0.52$). We then analyzed whether the transgene was expressed in β-cells by performing HA and insulin staining in pancreatic sections from TG and WT mice. As shown in Fig. 1E, HA was only detected in insulin-positive cells of TG mouse pancreas. Taken together, these data confirm the generation of TG mice with enhanced PKC-ζ activation in β-cells. For subsequent experiments, because of their similar levels of PKC-ζ overexpression and activation, data from the TG lines were pooled. In addition, similar numbers of male and female mice were analyzed per genotype.

TG mice display increased plasma insulin, improved glucose tolerance, and enhanced insulin secretion. Body weight and food intake were not significantly different between TG and WT mice (Supplementary Fig. 1). On the other hand, a significant increase in plasma insulin was observed in TG mice in both fasting and nonfasting conditions (Fig. 2A). This correlated with significantly diminished blood glucose in fasting conditions but normal blood glucose in nonfasting conditions (Fig. 2B), suggesting the activation of blood glucose regulatory mechanisms in the latter state. In addition, TG mice displayed improved glucose tolerance (Fig. 2C and D) without alteration in insulin sensitivity (Fig. 2E). These results suggest the possibility that TG mice have enhanced insulin secretion in vivo. Indeed, TG mice showed increased plasma insulin at baseline fasting conditions and also 5 min after glucose injection

fasted WT ($n = 7$) and TG ($n = 7$) littermates injected intraperitoneally with glucose (2 g/kg body wt). Blood was obtained before (basal, 0 min) and 5 min after glucose administration. Results are means ± SEM. Both at basal and 5 min after glucose administration, a significant increase in plasma insulin was observed in TG mice. *$P < 0.05$ vs. WT at 0 and 5 min and #$P < 0.05$ vs. the same genotype in basal conditions. (A high-quality color representation of this figure is available in the online issue.)
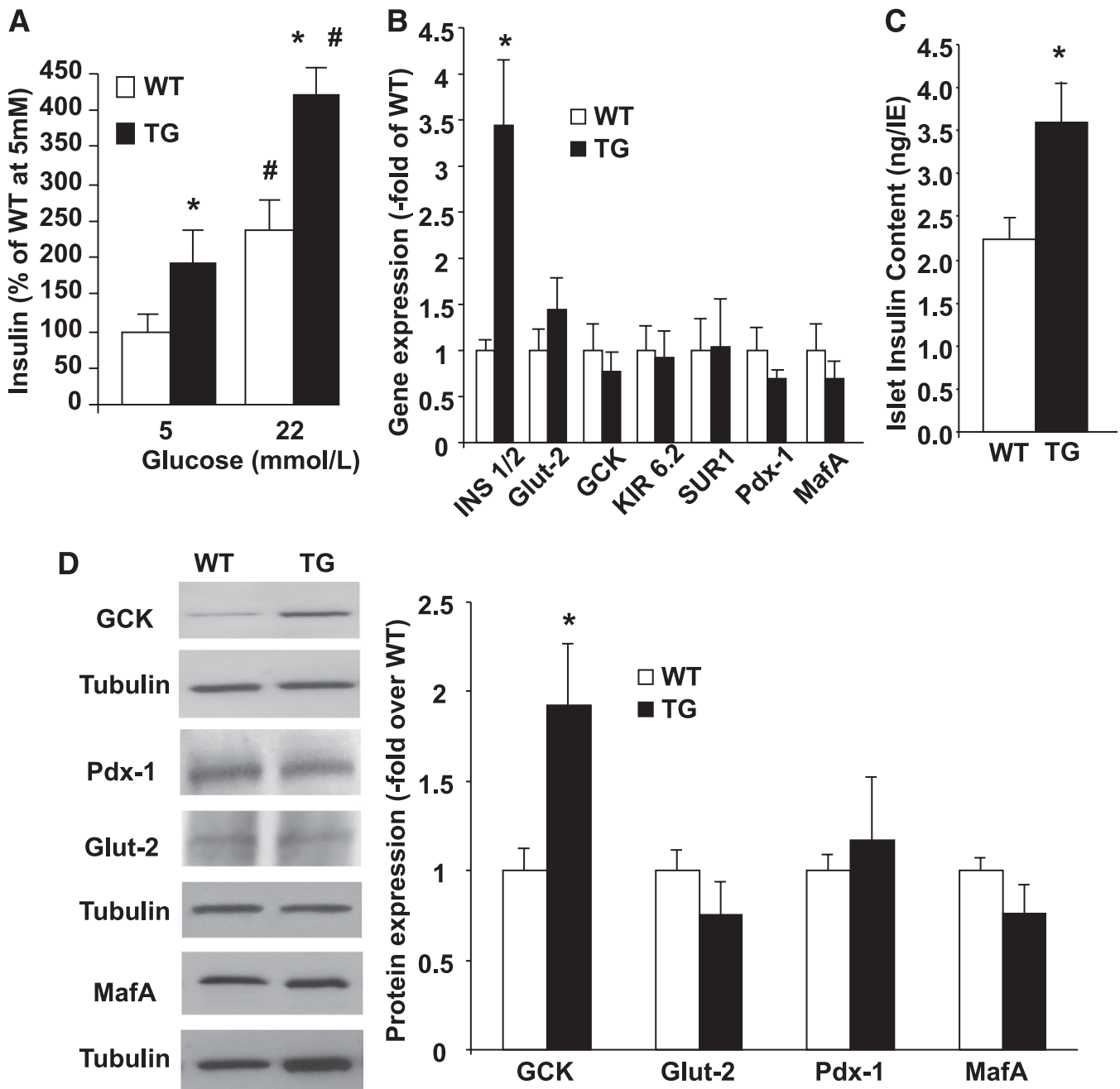
FIG. 3. Insulin secretion and expression analysis of functional markers in islets from RIP-CA-PKC-ζ mice. *A*: GSIS was performed in groups of 10 islets of similar sizes obtained from WT ($n = 6$) and TG ($n = 6$) mice and incubated for 30 min with 5 or 22 mmol/L glucose. Experiments were performed in triplicate, and insulin was measured by RIA. A significant increase in insulin secretion at 5 and 22 mmol/L glucose was observed in TG compared with WT islets. Results are means ± SEM. *$P < 0.05$ vs. WT at the same glucose concentration and #$P < 0.05$ vs. the same genotype at 5 mmol/L glucose. *B*: Real-time PCR analysis using specific primers (see Supplementary Table 1) for genes involved in insulin secretion and β-cell differentiation using total RNA extracted from islets isolated from at least $n = 3$ WT and at least $n = 3$ TG mice at 10–14 weeks of age. Mouse actin was used as a housekeeping gene. Results are means ± SEM. Only insulin mRNA expression was significantly increased in TG islets. *$P < 0.05$ vs. WT. *C*: Islet insulin content in aliquots of 50 IE isolated from 10- to 14-week-old WT ($n = 10$) and TG ($n = 6$) mice. Islet insulin content was significantly increased in TG islets. *$P < 0.05$ vs. WT. *D*: Expression of Glut-2, GCK, MafA, and Pdx-1 was assessed by Western blot of islet protein extracts from WT ($n = 6$) and TG ($n = 8$) mice at 10–14 weeks of age. Tubulin was used as an internal control for loading. A representative immunoblot using specific antibodies (Supplementary Table 2) is shown. Significantly increased levels of GCK were observed in TG mouse islets. *$P < 0.05$ vs. WT.

in the IPGTT experiments (Fig. 2*F*). Because TG mice had improved glucose tolerance and increased insulin secretion in vivo, we next assessed whether TG mouse islets display enhanced insulin secretory function ex vivo. As shown in Fig. 3*A*, TG islets under static incubation secreted significantly more insulin than WT islets at both 5 and 22 mmol/L glucose. Therefore, PKC-ζ activation in β-cells is accompanied by an improvement in β-cell function.

PKC-ζ activation leads to increased insulin mRNA, islet insulin content, and glucokinase expression. Because β-cell function was increased in TG islets, we next analyzed the expression of genes involved in insulin secretion. We found that insulin mRNA expression was significantly increased in TG islets without alteration in Glut-2, glucokinase (GCK), Kir6.2, SUR1 (Fig. 3*B*), voltage-dependent calcium channel (VDCC), syntaxin-1, or SNAP-25
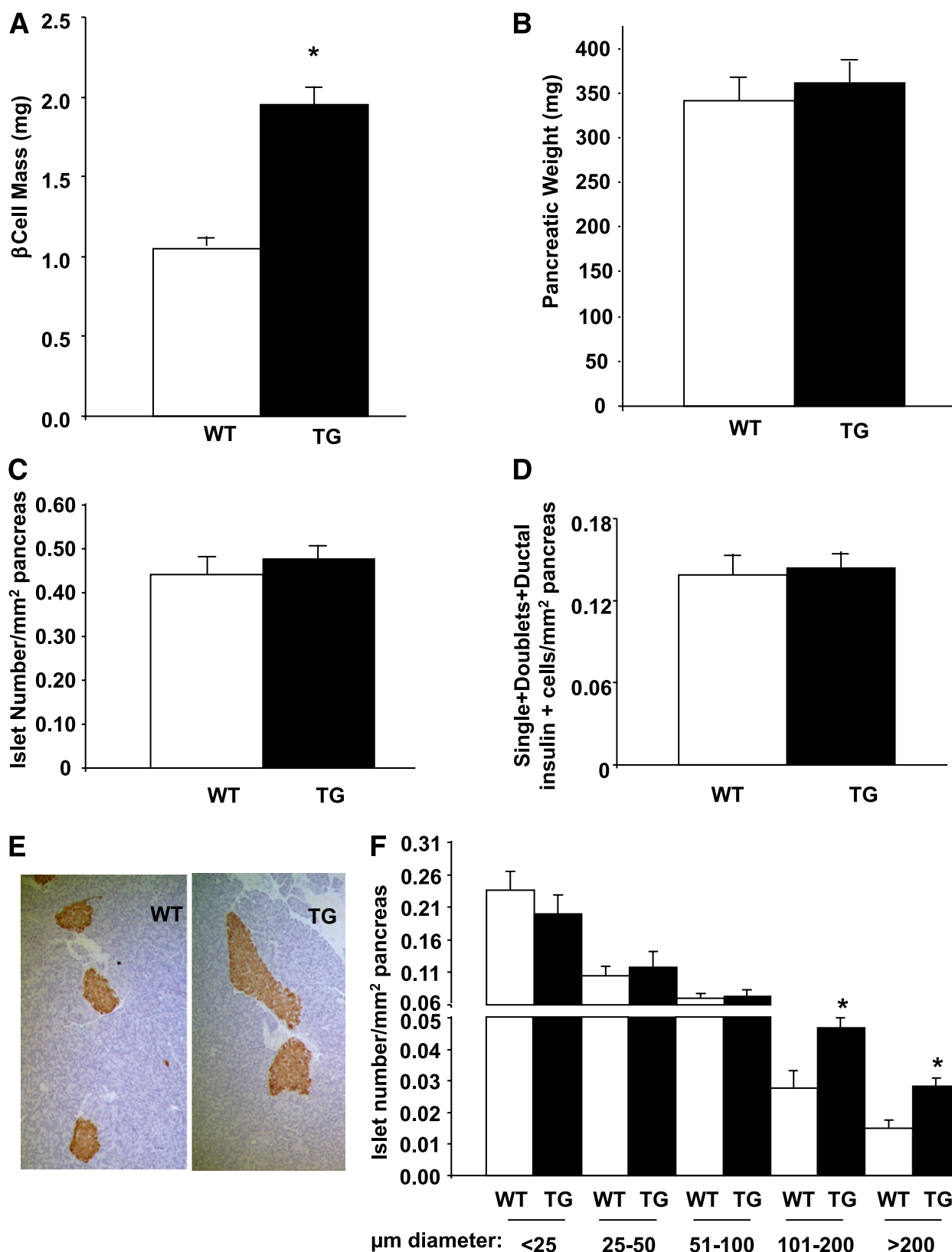
FIG. 4. Pancreas and islet histomorphometry in RIP-CA-PKC-ζ mice. Histomorphometry was performed in insulin-stained pancreatic sections from 12- to 14-week-old WT ($n = 11$) and TG ($n = 9$) littermates and β-cell mass (A), pancreas weight (B), islet number per pancreatic area (C), and number of single and double insulin-positive cells embedded in the acinar tissue and in ductal structures per pancreatic area (D) were measured. β-Cell mass was significantly increased in TG mice with no alteration in pancreas weight, islet number, or small clusters of insulin-positive cells. Results are means ± SEM. *$P < 0.05$ vs. WT. E: Representative microphotographs of WT and TG mouse pancreatic sections stained for insulin and counterstained with hematoxylin. TG mouse islets were increased in size compared with WT mice. F: Histomorphometric analysis of the islet size distribution per pancreatic area in pancreatic sections from WT and TG mice showed a significant increase in the number of islets with a diameter larger than 100 μm (larger islets) in TG mice. Results are means ± SEM and *$P < 0.05$ vs. WT of the same islet size. (A high-quality color representation of this figure is available in the online issue.)
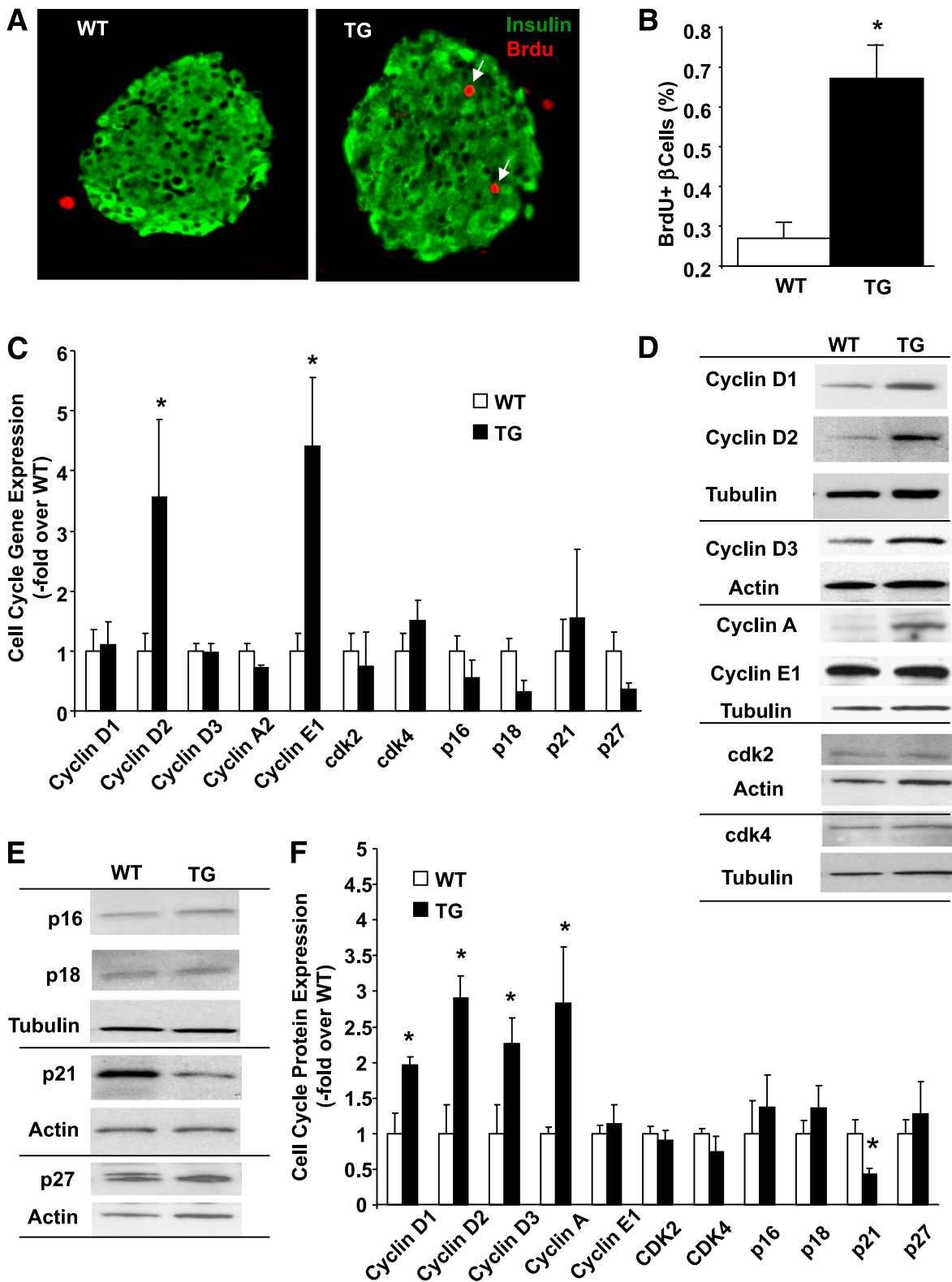
FIG. 5. β-Cell proliferation and cell cycle proteins in islets of RIP-CA-PKC-ζ mice. *A*: Representative microphotographs of insulin (green)- and BrdU (red)-stained pancreatic sections from 12- to 14-week-old WT and TG littermates. *B*: Quantification of the percentage of BrdU-positive β-cells in 12- to 14-week-old WT mice (*n* = 11) and TG (*n* = 9) littermates. BrdU incorporation in β-cells was significantly increased in TG mice compared with WT siblings. Results are means ± SEM. *$P < 0.05$ vs. WT. *C*: Expression of G1/S cell-cycle regulators by real-time PCR from islets isolated from 12- to 14-week-old WT mice (*n* = 8) and TG (*n* = 6) littermates. PCR cycles for each gene were compared with actin used as an internal control. The graph is depicted as fold-over control, with values from WT mouse islets taken as one. Results are means ± SEM. *$P < 0.05$ vs. WT. Western blot analysis of the G1/S cell-cycle activators (*D*) and inhibitors (*E*) from islets isolated from 12- to 14-week-old WT mice and TG littermates using actin or tubulin as the internal housekeeping protein control. *F*: Densitometric quantification of the level of these proteins in protein extracts from TG mouse islets (*n* = 8) compared with WT mice (*n* = 9). Results are means ± SEM. *$P < 0.05$ vs. WT. (A high-quality digital representation of this figure is available in the online issue.)
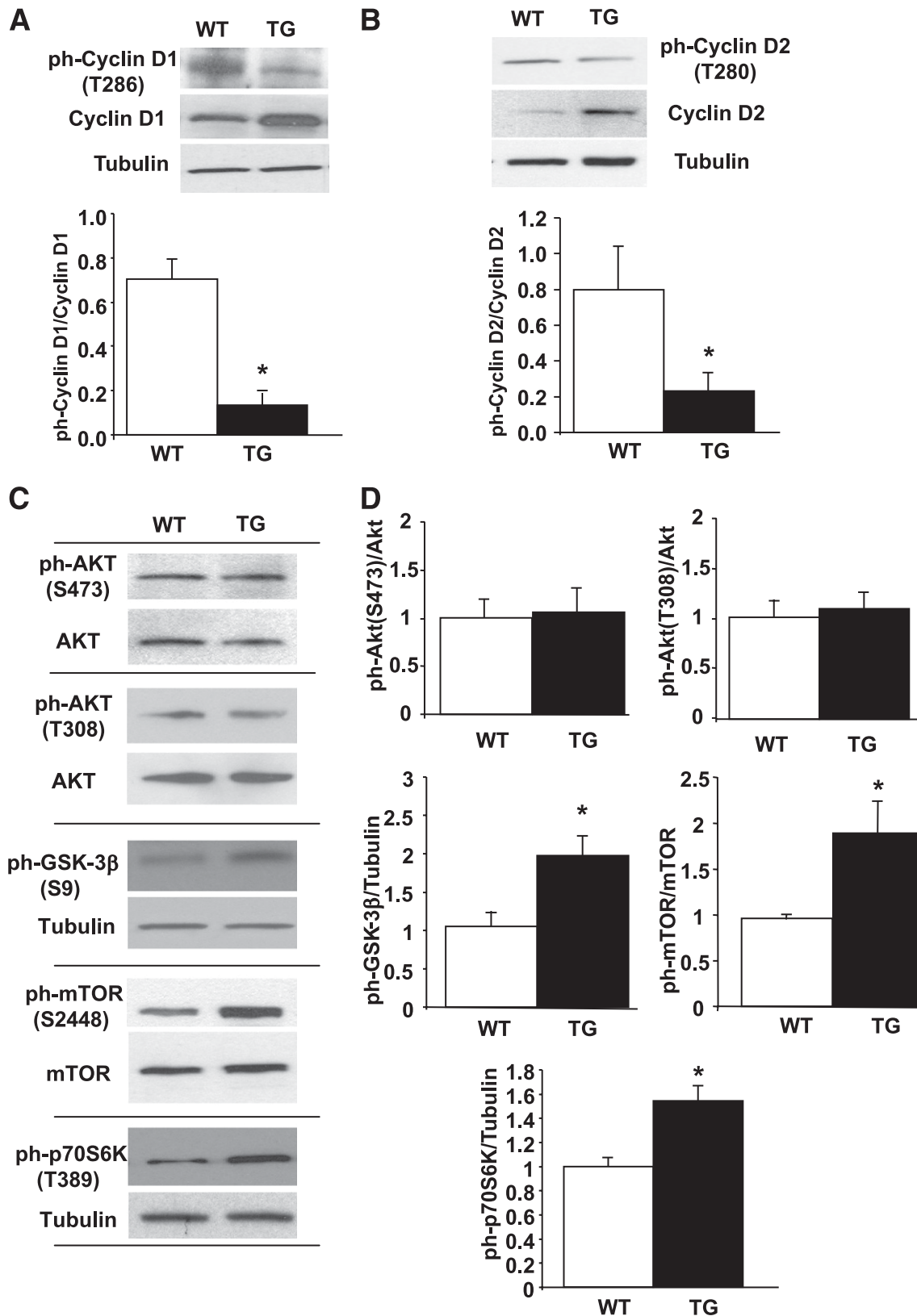
FIG. 6. Phosphorylation/activation of cell-cycle molecules and signaling pathways in RIP-CA-PKC-ζ mouse islets. Western blot analysis of the expression levels of phospho–Thr286-cyclin D1 (A) and phospho–Thr280-cyclin D2 (B) in islets isolated from 12- to 14-week-old WT mice and TG littermates using tubulin as the internal housekeeping protein control. Quantification of the ratios of phospho–Thr286-cyclin D1/cyclin D1 and phospho–Thr280-cyclin D2/cyclin D2 shows significant changes in these phospho-proteins in TG mouse islets ($n = 4$) compared with WT mice ($n = 4$). Results are means ± SEM and *$P < 0.05$ vs. WT. C: Representative Western blots of the expression levels of phospho-Ser473 and phospho–Thr308-Akt, phospho–Ser9-GSK-3β, phospho–Ser2448-mTOR, and phospho–Thr389-p70S6K in islets isolated from 12- to 14-week-old WT and TG littermates using Akt, mTOR, or tubulin as the internal housekeeping protein controls. D: Quantification of the ratios of these different phosphorylated forms of the signaling molecules mentioned in C shows significant changes in the phosphorylation of GSK-3β, mTOR, and p70S6K but not in Akt in TG ($n = 7$) compared with WT mouse islets ($n = 7$). The graph is depicted as fold-over control, with values from WT mouse islets taken as one. Results are means ± SEM. *$P < 0.05$ vs. WT.
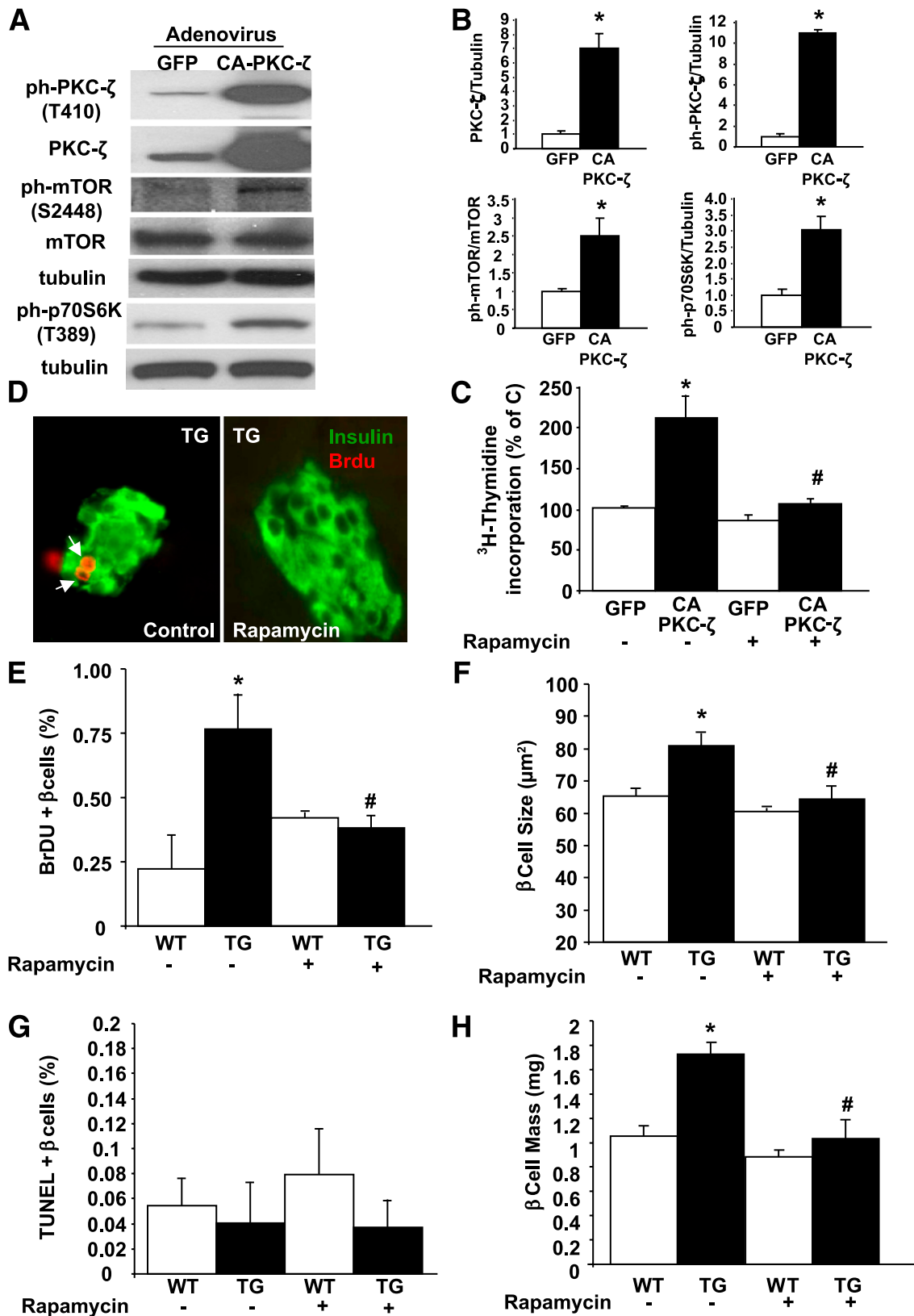
FIG. 7. Rapamycin inhibits the increase in β-cell proliferation and mass induced by CA-PKC-ζ. *A*: Representative Western blot of protein extracts from INS-1 cells transduced with 100 MOI of adenovirus containing CA-PKC-ζ or GFP cDNAs for 24 h showing that the increased expression and phosphorylation of PKC-ζ correlates with increased phosphorylation of mTOR and its downstream target, p70S6K. *B*: Densitometric quantification of the level of these proteins in four different experiments. Results are means ± SEM. *$P < 0.05$ vs. GFP. *C*: Effect of 10 nmol/L rapamycin on CA-PKC-ζ–induced cell proliferation measured by [³H]thymidine incorporation in INS-1 cells transduced with the adenoviruses indicated in *A*. Values are means ± SE of four experiments in triplicate. *$P < 0.05$ vs. GFP with no inhibitors; #$P < 0.05$ vs. CA-PKC-ζ with no inhibitors. *D*: Effect of 0.5 mg/kg body wt i.p. administration of rapamycin for 14 days on β-cell proliferation in TG mice and WT littermates measured by BrdU incorporation. Representative microphotographs of insulin (green)- and BrdU (red)-stained pancreatic sections from 12- to 14-week-old TG mice treated with

mRNA (not shown). This increase in insulin mRNA translated to a significant increase in islet insulin content (Fig. 3C). Interestingly, the expression of transcription factors involved in insulin gene expression such as Pdx-1 and MafA was normal in TG islets (Fig. 3B and D), suggesting the involvement of other transcription factors or increase in DNA-binding activity of Pdx-1 or MafA as potential mechanisms involved in insulin mRNA upregulation. However, although GCK mRNA was not altered, GCK protein was significantly increased in TG islets (Fig. 3D), suggesting that upregulation of both insulin and GCK expression could be involved in the increased insulin secretion.

Activation of PKC-ζ in β-cells increases islet size and β-cell mass. To determine whether the metabolic improvement in TG mice correlated with changes in β-cell homeostasis, we measured β-cell mass in these mice. β-Cell mass was significantly increased in 12- to 14-week-old TG mice (Fig. 4A) without changes in pancreatic weight, total islet number, or the number of small islets (single and doublet β-cells) or insulin-positive cells in ducts (Fig. 4B–D). Islet size was visibly increased (Fig. 4E), and the number of large islets (>100 μm diameter) was almost double (Fig. 4F) in TG mice, suggesting that the enhanced β-cell mass was due to an increase in the number of larger islets. Interestingly, β-cell mass in TG mice was not significantly enhanced at 1 week of age but was significantly increased at 6 weeks of age (Supplementary Fig. 2A and C), suggesting enhancement of β-cell mass at early maturity and adulthood but not at early postnatal ages.

PKC-ζ activation increases β-cell proliferation in vivo, upregulates cyclin Ds and A, and decreases p21. Analysis of in vivo β-cell proliferation was assessed by quantifying BrdU incorporation into β-cells of WT and TG mouse pancreatic sections. TG mouse pancreata from 12- to 14-week-old mice displayed increased BrdU incorporation into β-cells (Fig. 5A), and quantification of β-cell replication in several sections from these mice revealed a significant increase compared with WT siblings (Fig. 5B). This increase in β-cell proliferation was already present at 1 and 6 weeks of age (Supplementary Fig. 2B and D).

The proliferative capacity of β-cells decreases with age (21,22). We determined whether acute activation of PKC-ζ could also increase β-cell proliferation in islet cell cultures from aged mice. As previously shown in β-cells from young mice (3), Adv-CA-PKC-ζ also significantly enhanced β-cell replication in islet cells from 1-year-old mice (Supplementary Fig. 3).

Because PKC-ζ activation leads to increased β-cell proliferation, we sought to determine whether PKC-ζ alters cell cycle gene and protein expression in TG islets. Real-time PCR analysis revealed a 3- to 4-fold increase in cyclins D2 and E1 mRNA expression without significant alteration in other cell cycle genes regulating the G1/S transition (cyclins D1, D3, and A2 and cdk-2, cdk-4, p16, p18, p21, and p27) (Fig. 5C). The increase in cyclin D2 mRNA was accompanied by a significant increase in cyclin D2 protein. Interestingly, the two other D-cyclins, D1 and D3, were also increased at the protein level (Fig. 5D and F). Although cyclin E1 mRNA was upregulated, no alteration in protein levels was observed in TG islets (Fig. 5C, D, and

F). On the other hand, cyclin A protein was significantly increased in TG islets (Fig. 5D and F). No significant changes were found in cdk-2 and cdk-4 levels (Fig. 5D and F). Analysis of cell-cycle inhibitors revealed that p21 was significantly decreased in TG islets (Fig. 5E and F). No alterations were found in p16, p18, or p27 (Fig. 5E and F). Taken together, these results indicate that PKC-ζ activation in β-cells of TG mice leads to upregulation of the G1/S cell cycle activators D-cyclins and cyclin A and downregulation of the cell-cycle inhibitor p21, likely driving the increased β-cell replication.

Phosphorylation of Thr residues in the COOH terminus of D-cyclins is a known signal for their degradation by an ubiquitin-dependent mechanism (23–25). Because cyclins D1 and D2 are the most highly expressed in mouse islets (26) and are upregulated in TG islets, we determined the levels of phospho–Thr286-cyclin D1 and phospho–Thr280-cyclin D2 in TG and WT islets. As shown in Fig. 6A and B, phospho–Thr286 cyclin D1 and phospho–Thr280 cyclin D2 levels were significantly decreased in TG islets. Of note, it has been reported that antibodies against phospho–Thr286-cyclin D1 can recognize phospho–Thr280-cyclin D2; therefore, it is possible that the diminished phosphorylation observed in TG islets reflects only a decrease in Thr280 cyclin D2 and not in both D-cyclins (24,27). Nevertheless, these studies suggest that PKC-ζ activation leads to decreased Thr phosphorylation in D-cyclins, potentially resulting in decreased degradation and enhanced accumulation in TG mouse islets.

GSK-3β and mTOR are phosphorylated in TG mouse islets. GSK-3β has been reported to phosphorylate D-cyclins on Thr residues facilitating nuclear exclusion and targeting for proteosomal degradation (23–25). Because D-cyclins were upregulated and their phosphorylation was downregulated in TG islets, we wondered whether GSK-3β inactivation (increased phosphorylation) was enhanced in these islets. As shown in Fig. 6C and D, GSK-3β inactivation was significantly enhanced in TG islets. Furthermore, recent reports indicate that mTOR activation regulates cyclin D2 stability in β-cells (28). Because cyclin D2 is upregulated in TG islets and mTOR is a downstream target of PKC-ζ in follicular lymphoma cells (12), we wondered whether mTOR activation was increased in TG mouse islets. Indeed, phosphorylation of mTOR and its downstream target p70S6K was significantly increased in these islets (Fig. 6C and D). Interestingly, Akt phosphorylation on Ser473 and Thr308 was not altered (Fig. 6C and D), suggesting that GSK-3β inactivation and mTOR activation were not mediated by Akt. In addition, ERK1/2 phosphorylation and the levels of IRS2, p85-PI3K, ERK1/2, or PDK-1 were not altered in TG mouse islets (not shown).

Rapamycin treatment abolishes the increase in β-cell replication and size and the improvement in glucose tolerance induced by PKC-ζ. We next analyzed whether mTOR activation is required for the proliferative effects of PKC-ζ in β-cells. As shown in Fig. 7A–C, INS-1 cells transduced with Adv-CA-PKC-ζ displayed increased PKC-ζ activation, enhanced mTOR phosphorylation and activity, and increased cell replication. Interestingly, treatment with rapamycin completely inhibited the Adv-CA-PKC-ζ–mediated

rapamycin (right) or the same volume of vehicle (0.4% DMSO) (*left panel*). Quantification of β-cell proliferation (*E*), size (*F*), death (*G*), and mass (*H*) in 12- to 14-week-old mice injected with vehicle (WT = 7; TG = 7) or 0.5 mg/kg body wt rapamycin (WT = 7; TG = 9) for 14 days. Pancreatic sections were stained as indicated in RESEARCH DESIGN AND METHODS. β-Cell replication, size, and mass were significantly increased in TG mice compared with WT siblings injected with vehicle. The increases were blunted by the administration of rapamycin. Results are means ± SEM. *P < 0.05 vs. WT vehicle; #P < 0.05 vs. TG vehicle. (A high-quality digital representation of this figure is available in the online issue.)
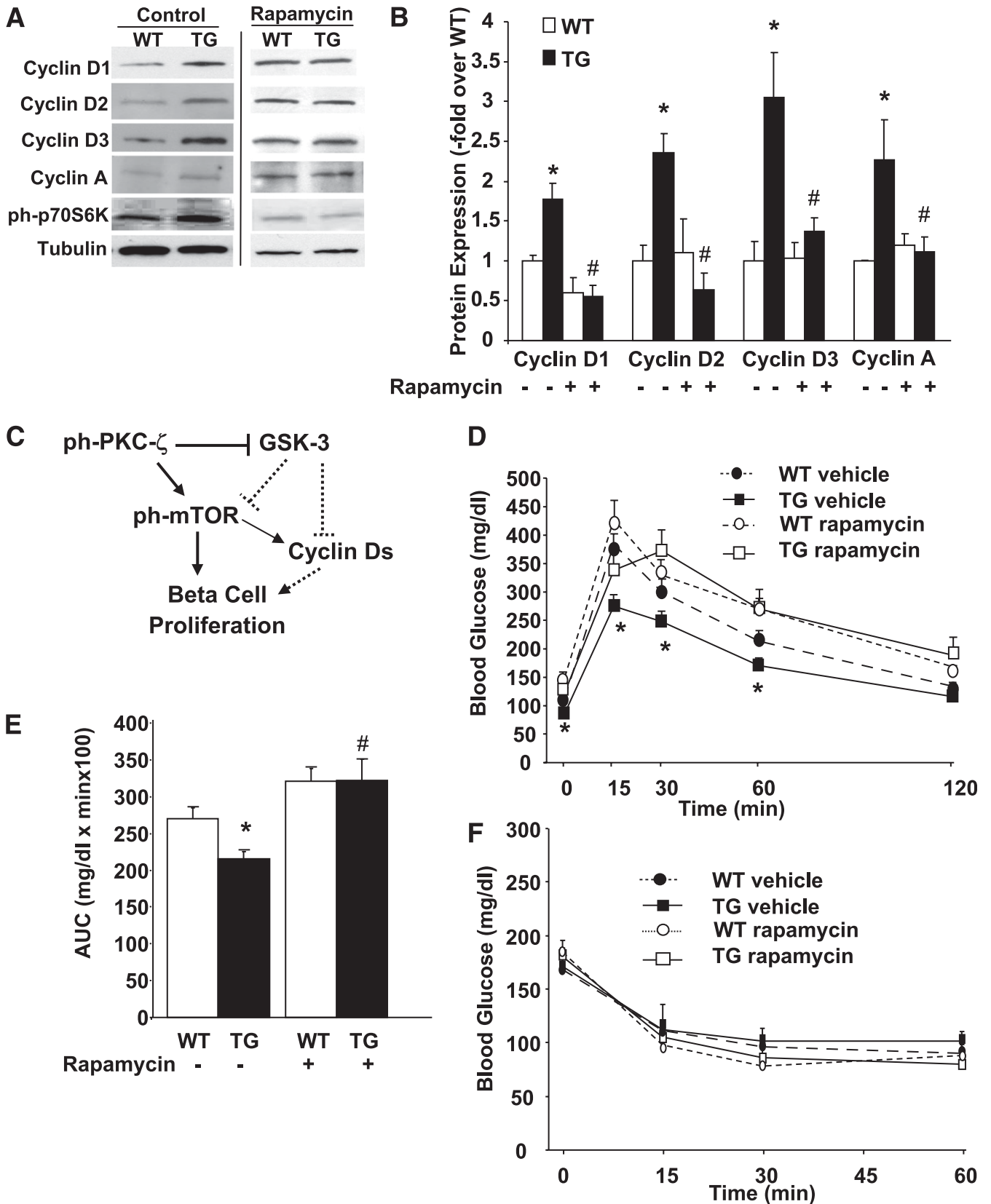
FIG. 8. Rapamycin decreases the expression of cyclins D1, D2, D3, and A in RIP-CA-PKC-ζ islets. *A*: Representative Western blots of cyclins D1, D2, D3, and A, and phospho–Thr387-p70S6K in islets isolated from 12- to 14-week-old WT mice and TG littermates treated with vehicle (0.4% DMSO, control) or 0.5 mg/kg body wt rapamycin for 14 days using tubulin as the internal housekeeping protein control. *B*: Quantitation of the ratio of cyclins D1, D2, D3, and A to tubulin shows significant increases in these proteins in TG mouse islets ($n = 5$) compared with WT mice ($n = 6$) treated with vehicle. This increase was blunted in TG mouse islets ($n = 5$) compared with WT mice ($n = 6$) following administration of rapamycin. Results are means ± SEM. *$P < 0.05$ vs. WT vehicle; #$P < 0.05$ vs. TG vehicle. *C*: Schematic representation of a model for the mitogenic signaling pathways induced by CA-PKC-ζ in the β-cell. Broken lines denote potential regulatory pathways. IPGTT (*D*) and areas under the curve (AUCs) (*E*)

increase in INS-1 cell proliferation (Fig. 7C). To address whether mTOR activation is essential for CA-PKC-ζ–mediated β-cell proliferation in vivo, we treated TG and WT mice with rapamycin for 14 days. As shown in Fig. 7D and E, BrdU incorporation in β-cells was decreased in TG mice treated with rapamycin reaching levels similar to WT mice. In addition, β-cell size was significantly increased in TG mice, and this increase was abolished by rapamycin (Fig. 7F). On the other hand, no significant changes in β-cell death were observed in these mice 2 weeks after the treatment (Fig. 7G). Importantly, rapamycin also decreased β-cell mass in TG mice to levels similar to those seen in WT mice (Fig. 7H), suggesting that the decrease in β-cell proliferation and size and a potential undetected increase in β-cell death induced by rapamycin counteract the effects of CA-PKC-ζ on β-cell expansion.

As expected, rapamycin treatment blocked the upregulation of phospho–p70S6K in TG islets (Fig. 8A). More importantly, rapamycin eliminated the upregulation of cyclins Ds and A in TG islets (Fig. 8A and B). Collectively, these results show that mTOR activation is a critical downstream signal mediating PKC-ζ–driven β-cell proliferation and size and the upregulation of cell-cycle activators that increase β-cell mass (Fig. 8C). In addition, rapamycin treatment eliminated the improved glucose tolerance in TG mice (Fig. 8D and E), suggesting that the effects on glucose homeostasis were also mTOR dependent. TG and WT mice treated with vehicle or rapamycin for 2 weeks responded similarly in ITT experiments (Fig. 8F), suggesting that although this dose of rapamycin blocks mTOR activity (Fig. 8A), it does not grossly affect insulin sensitivity in these mice, as previously shown in studies using a similar dose of rapamycin (29).

DISCUSSION

This study provides the first direct evidence that PKC-ζ activation increases β-cell proliferation, size, and mass in vivo. These beneficial effects are accompanied by significantly improved glucose tolerance and enhanced insulin expression and secretion. Therefore, these observations identify the atypical PKC-ζ pathway as a therapeutic target for the treatment of diabetes.

The PKC-ζ–induced β-cell replication was associated with upregulation of D-cyclins and cyclin A and downregulation of the cyclin-dependent kinase inhibitor p21. It has been shown that cyclin D1 overexpression in rat and human islets in vitro and in the β-cell of TG mice in vivo increases β-cell proliferation and mass (30). Similarly, overexpression of either cyclin D2 or A also enhances β-cell proliferation in vitro (31,32). Cyclin D2 is essential for postnatal β-cell growth and the compensatory β-cell hyperplastic response to insulin resistance in rodents (26,33), and cyclin A is essential for exendin-4–mediated β-cell proliferation (32). Furthermore, p21-null islets display increased growth factor–induced β-cell replication (34). Collectively, these studies support the notion that the PKC-ζ–induced β-cell replication in vivo results from alterations in D-cyclin, cyclin A and p21 expression leading to the acceleration of the G1/S transition of the cell cycle.

Cyclins D1, D2, and D3 are targeted for proteosomal degradation by phosphorylation on Thr286, Thr280, and Thr283, respectively (23–25). Islets expressing CA-PKC-ζ

displayed diminished phosphorylation of Thr residues at D-cyclins, suggesting that their increased expression could be due to diminished degradation by the ubiquitin/proteasome-dependent mechanism. In addition, phosphorylation of these Thr residues in D-cyclins redirect these proteins from the nucleus to the cytoplasm (23,27), suggesting that islets expressing CA-PKC-ζ might have increased nuclear localization of cyclin Ds. GSK-3β is one of the kinases known to phosphorylate D-cyclins on these Thr and to regulate their degradation (23–25). PKC-ζ is a natural kinase of GSK-3 in Xenopus embryos and mammalian skeletal muscle cells, leading to its inactivation (12,35). However, whether GSK-3 is downstream of PKC-ζ in β-cells is unknown. In this study, we find that PKC-ζ activation indeed results in increased GSK-3β phosphorylation/inactivation, which could explain the decreased phosphorylation and increased accumulation of D-cyclins. Whether this is the case for cyclin A warrants further studies, although to our knowledge the involvement of GSK-3 in cyclin A degradation has previously not been described. In addition, it has been reported that activation of PKC-ζ decreases p21 half-life in HeLa cells (36). Although the mechanism involved in this decrease is unclear, it could be mediated by phosphorylation at Ser146, which has been suggested to both increase its degradation and/or impair its nuclear translocation and action as a cdk inhibitor (36,37).

mTOR plays a pivotal role in cell metabolism, growth, and proliferation (38,39). mTOR nucleates two distinct multiprotein complexes: mTOR complex 1 (mTORC1) and 2 (mTORC2) (40,41). mTORC1 is sensitive to rapamycin and is a major modulator of cell-cycle progression in β-cells by regulating the levels of D-cyclins (28,42). Rapamycin has been shown to inhibit β-cell proliferation in vitro and in vivo and to downregulate growth factor–induced D-cyclin expression (29,42,43). In follicular lymphoma cells, PKC-ζ inhibition leads to decreased mTOR activity, suggesting that PKC-ζ regulates mTOR in these cells (13). The current study is the first to demonstrate that PKC-ζ activation in β-cells in vivo causes phosphorylation and activation of mTOR without increased phosphorylation/activation of Akt, a known activator of mTOR. This suggests that PKC-ζ can activate mTOR without stimulation of Akt and that mTORC1 but not mTORC2 (a kinase of Ser473 in Akt) is the complex activated by PKC-ζ. Indeed, in vivo rapamycin treatment eliminated the PKC-ζ–mediated mTOR activity (p70S6K phosphorylation) and, more importantly, the increase in β-cell proliferation, size, and mass; the upregulation of cyclins Ds and A; and the improved glucose tolerance—suggesting that mTORC1 activation is required for these PKC-ζ–induced effects. Although we did not observe an increase in β-cell death after 2 weeks of rapamycin treatment, a potential earlier undetected increase in β-cell death might contribute to the normalization of β-cell mass in TG mice. The analysis of PKC-ζ–mediated regulation of mTOR warrants further studies. It has been shown that GSK-3 can inhibit mTOR via phosphorylation of tuberin (Tsc2) (44). Tsc2 forms a complex with hamartin (Tsc1), and disruption of Tsc2 in β-cells increases β-cell proliferation and mass in an mTORC1-dependent manner (19). Therefore, inactivation of GSK-3β by PKC-ζ could be responsible for the enhancement of mTOR activity in TG islets.

---

calculated from these results and insulin tolerance test (F) performed in nonfasting 12- to 14-week-old mice injected with vehicle (WT = 7; TG = 7) or 0.5 mg/kg body wt rapamycin (WT = 7; TG = 9) for 14 days. No significant differences were found in blood glucose levels before or after insulin administration in both types of mice. Values are means ± SEM. *$P < 0.05$ vs. WT vehicle.

One might predict that the increase in β-cell proliferation in TG mouse islets could lead to diminished β-cell differentiation and insulin secretion. On the other hand, in vitro studies suggest that PKC-ζ activation might be required for GSIS (6,7) and that enhanced PKC-ζ activation could lead to increased insulin secretion. Our current studies find no negative functional impact of the proliferation state, given that TG mice displayed increased circulating insulin in fasting and nonfasting conditions and enhanced insulin secretion after a challenge with glucose. Furthermore, in vitro experiments confirmed that insulin secretion was enhanced in CA-PKC-ζ–expressing islets. In addition, CA-PKC-ζ expression in islets led to insulin mRNA and protein upregulation and enhanced glucokinase expression. It has been suggested that PKC-ζ may increase Pdx-1 DNA-binding activity and transcriptional activation of the insulin gene promoter in β-cells treated with stimulating concentrations of glucose (5). However, whether this is the case in TG mouse β-cells is unknown and warrants further studies. On the other hand, the increase in glucokinase expression in TG islets is not associated with increased mRNA, suggesting that posttranslational modifications induced by PKC-ζ might lead to glucokinase accumulation. Glucokinase is the rate-limiting enzyme for GSIS, and overexpression of glucokinase in β-cells leads to modest increases (30–60%) in insulin secretion at low and high glucose concentrations (45). Therefore, the increase in glucokinase and insulin content in TG islets could be responsible for the observed increase in insulin secretion. Taken together, these studies indicate a beneficial effect of PKC-ζ activation in β-cell function in vivo, highlighting the potential value of PKC-ζ activation in therapies not only oriented toward increasing β-cell regeneration but also toward enhancing insulin secretion.

Recent studies on ROSA26 reporter mice indicate that transgene expression is present in the brain of TG mice generated with RIP-II (46). In our study, phospho–PKC-ζ levels in brain protein extracts from TG and WT mice were not significantly different by immunoblot. However, this method is probably not sensitive enough to detect mild transgene expression in regions of the brain; therefore, it is very likely that expression in the brain could also be present in these TG mice. The impact of this potential nontargeted expression of the transgene in the phenotype of the TG mice is unknown. However, we have observed that CA-PKC-ζ overexpression leads to enhanced β-cell proliferation in INS-1 cells, mouse, and human islets in vitro (3), an aspect also seen in TG mice. In addition, we have found that the increase in proliferation is mediated by mTOR in vitro—an aspect also observed in vivo, where rapamycin blocks the increase in β-cell proliferation and mass in TG mice. In addition, insulin secretion in isolated TG islets ex vivo, outside of the influence of the nervous system, is enhanced, suggesting that PKC-ζ activation in β-cells can increase insulin secretion and improve glucose tolerance. Importantly, body weight, food intake, and insulin sensitivity tests were very similar between WT and TG mice. Taken together, these findings strongly suggest a cell-autonomous effect of PKC-ζ activation on β-cell function and proliferation.

In summary, this study provides novel evidence of the beneficial effects of PKC-ζ activation in β-cell proliferation, mass, and function in vivo. Elimination of these effects by rapamycin demonstrates that mTOR is a novel and important downstream mediator of PKC-ζ actions in the β-cell. In addition, acute activation of PKC-ζ also increases proliferation of β-cells from older mice. Collectively, these studies suggest a promising therapeutic future for this pathway in the treatment of diabetes.

REFERENCES

1. Hirai T, Chida K. Protein kinase Czeta (PKCzeta): activation mechanisms and cellular functions. J Biochem 2003;133:1–7
2. Chou MM, Hou W, Johnson J, et al. Regulation of protein kinase C ζ by PI 3-kinase and PDK-1. Curr Biol 1998;8:1069–1077
3. Vasavada RC, Wang L, Fujinaka Y, et al. Protein kinase C-zeta activation markedly enhances beta-cell proliferation: an essential role in growth factor mediated beta-cell mitogenesis. Diabetes 2007;56:2732–2743
4. Buteau J, Foisy S, Rhodes CJ, Carpenter L, Biden TJ, Prentki M. Protein kinase Czeta activation mediates glucagon-like peptide-1-induced pancreatic beta-cell proliferation. Diabetes 2001;50:2237–2243
5. Furukawa N, Shirotani T, Araki E, et al. Possible involvement of atypical protein kinase C (PKC) in glucose-sensitive expression of the human insulin gene: DNA-binding activity and transcriptional activity of pancreatic and duodenal homeobox gene-1 (PDX-1) are enhanced via calphostin C-sensitive but phorbol 12-myristate 13-acetate (PMA) and Gö 6976-insensitive pathway. Endocr J 1999;46:43–58
6. Harris TE, Persaud SJ, Jones PM. Atypical isoforms of pKc and insulin secretion from pancreatic beta-cells: evidence using Gö 6976 and Ro 31-8220 as Pkc inhibitors. Biochem Biophys Res Commun 1996;227:672–676
7. Miele C, Raciti GA, Cassese A, et al. PED/PEA-15 regulates glucose-induced insulin secretion by restraining potassium channel expression in pancreatic beta-cells. Diabetes 2007;56:622–633
8. Wrede CE, Dickson LM, Lingohr MK, Briaud I, Rhodes CJ. Fatty acid and phorbol ester-mediated interference of mitogenic signaling via novel protein kinase C isoforms in pancreatic beta-cells (INS-1). J Mol Endocrinol 2003;30:271–286
9. Hennige AM, Fritsche A, Strack V, et al. PKC ζ enhances insulin-like growth factor 1-dependent mitogenic activity in the rat clonal beta cell line RIN 1046-38. Biochem Biophys Res Commun 2002;290:85–90
10. Berra E, Diaz-Meco MT, Dominguez I, et al. Protein kinase C ζ isoform is critical for mitogenic signal transduction. Cell 1993;74:555–563
11. Diaz-Meco MT, Moscat J. MEK5, a new target of the atypical protein kinase C isoforms in mitogenic signaling. Mol Cell Biol 2001;21:1218–1227
12. Ossipova O, Bardeesy N, DePinho RA, Green JB. LKB1 (XEEK1) regulates Wnt signalling in vertebrate development. Nat Cell Biol 2003;5:889–894
13. Leseux L, Laurent G, Laurent C, et al. PKC zeta mTOR pathway: a new target for rituximab therapy in follicular lymphoma. Blood 2008;111:285–291
14. Romanelli A, Martin KA, Toker A, Blenis J. p70 S6 kinase is regulated by protein kinase Czeta and participates in a phosphoinositide 3-kinase-regulated signalling complex. Mol Cell Biol 1999;19:2921–2928
15. Garcia-Ocaña A, Takane KK, Syed MA, Philbrick WM, Vasavada RC, Stewart AF. Hepatocyte growth factor overexpression in the islet of transgenic mice increases beta cell proliferation, enhances islet mass, and induces mild hypoglycemia. J Biol Chem 2000;275:1226–1232

16. Kohout TA, Rogers TB. Use of a PCR-based method to characterize protein kinase C isoform expression in cardiac cells. Am J Physiol 1993;264:C1350–C1359

17. Roccisana J, Reddy V, Vasavada RC, Gonzalez-Pertusa JA, Magnuson MA, Garcia-Ocaña A. Targeted inactivation of hepatocyte growth factor receptor c-met in beta-cells leads to defective insulin secretion and GLUT-2 downregulation without alteration of beta-cell mass. Diabetes 2005;54:2090–2102

18. Rao P, Roccisana J, Takane KK, et al. Gene transfer of constitutively active Akt markedly improves human islet transplant outcomes in diabetic SCID mice. Diabetes 2005;54:1664–1675

19. Rachdi L, Balcazar N, Osorio-Duque F, et al. Disruption of Tsc2 in pancreatic beta cells induces beta cell mass expansion and improved glucose tolerance in a TORC1-dependent manner. Proc Natl Acad Sci USA 2008;105:9250–9255

20. Bachmanov AA, Reed DR, Beauchamp GK, Tordoff MG. Food intake, water intake, and drinking spout side preference of 28 mouse strains. Behav Genet 2002;32:435–443

21. Tschen SI, Dhawan S, Gurlo T, Bhushan A. Age-dependent decline in beta-cell proliferation restricts the capacity of beta-cell regeneration in mice. Diabetes 2009;58:1312–1320

22. Rankin MM, Kushner JA. Adaptive beta-cell proliferation is severely restricted with advanced age. Diabetes 2009;58:1365–1372

23. Diehl JA, Cheng M, Roussel MF, Sherr CJ. Glycogen synthase kinase-3beta regulates cyclin D1 proteolysis and subcellular localization. Genes Dev 1998;12:3499–3511

24. Kida A, Kakihana K, Kotani S, Kurosu T, Miura O. Glycogen synthase kinase-3beta and p38 phosphorylate cyclin D2 on Thr280 to trigger its ubiquitin/proteasome-dependent degradation in hematopoietic cells. Oncogene 2007;26:6630–6640

25. Naderi S, Gutzkow KB, Låhne HU, et al. cAMP-induced degradation of cyclin D3 through association with GSK-3beta. J Cell Sci 2004;117:3769–3783

26. Kushner JA, Ciemerych MA, Sicinska E, et al. Cyclins D2 and D1 are essential for postnatal pancreatic beta-cell growth. Mol Cell Biol 2005;25:3752–3762

27. He LM, Sartori DJ, Teta M, et al. Cyclin D2 protein stability is regulated in pancreatic β-cells. Mol Endocrinol 2009;23:1865–1875

28. Balcazar N, Sathyamurthy A, Elghazi L, et al. mTORC1 activation regulates beta-cell mass and proliferation by modulation of cyclin D2 synthesis and stability. J Biol Chem 2009;284:7832–7842

29. Zahr E, Molano RD, Pileggi A, et al. Rapamycin impairs in vivo proliferation of islet beta-cells. Transplantation 2007;84:1576–1583

30. Zhang X, Gaspard JP, Mizukami Y, Li J, Graeme-Cook F, Chung DC. Overexpression of cyclin D1 in pancreatic beta-cells in vivo results in islet hyperplasia without hypoglycemia. Diabetes 2005;54:712–719

31. Fiaschi-Taesch NM, Salim F, Kleinberger J, et al. Induction of human beta-cell proliferation and engraftment using a single G1/S regulatory molecule, cdk6. Diabetes 2010;59:1926–1936

32. Song WJ, Schreiber WE, Zhong E, et al. Exendin-4 stimulation of cyclin A2 in beta-cell proliferation. Diabetes 2008;57:2371–2381

33. Georgia S, Hinault C, Kawamori D, et al. Cyclin D2 is essential for the compensatory beta-cell hyperplastic response to insulin resistance in rodents. Diabetes 2010;59:987–996

34. Cozar-Castellano I, Weinstock M, Haught M, Velázquez-Garcia S, Sipula D, Stewart AF. Evaluation of beta-cell replication in mice transgenic for hepatocyte growth factor and placental lactogen: comprehensive characterization of the G1/S regulatory proteins reveals unique involvement of p21cip. Diabetes 2006;55:70–77

35. Oriente F, Formisano P, Miele C, et al. Insulin receptor substrate-2 phosphorylation is necessary for protein kinase C zeta activation by insulin in L6hIR cells. J Biol Chem 2001;276:37109–37119

36. Scott MT, Ingram A, Ball KL. PDK1-dependent activation of atypical PKC leads to degradation of the p21 tumour modifier protein. EMBO J 2002;21:6771–6780

37. Child ES, Mann DJ. The intricacies of p21 phosphorylation: protein/protein interactions, subcellular localization and stability. Cell Cycle 2006;5:1313–1319

38. Guertin DA, Sabatini DM. Defining the role of mTOR in cancer. Cancer Cell 2007;12:9–22

39. Wullschleger S, Loewith R, Hall MN. TOR signaling in growth and metabolism. Cell 2006;124:471–484

40. Kim DH, Sarbassov DD, Ali SM, et al. mTOR interacts with raptor to form a nutrient-sensitive complex that signals to the cell growth machinery. Cell 2002;110:163–175

41. Sarbassov DD, Ali SM, Kim DH, et al. Rictor, a novel binding partner of mTOR, defines a rapamycin-insensitive and raptor-independent pathway that regulates the cytoskeleton. Curr Biol 2004;14:1296–1302

42. Aronovitz A, Josefson J, Fisher A, et al. Rapamycin inhibits growth factor-induced cell cycle regulation in pancreatic beta cells. J Investig Med 2008;56:985–996

43. Liu H, Remedi MS, Pappan KL, et al. Glycogen synthase kinase-3 and mammalian target of rapamycin pathways contribute to DNA synthesis, cell cycle progression, and proliferation in human islets. Diabetes 2009;58:663–672

44. Rosner M, Hanneder M, Siegel N, Valli A, Hengstschläger M. The tuberous sclerosis gene products hamartin and tuberin are multifunctional proteins with a wide spectrum of interacting partners. Mutat Res 2008;658:234–246

45. Becker TC, Noel RJ, Johnson JH, et al. Differential effects of overexpressed glucokinase and hexokinase I in isolated islets. Evidence for functional segregation of the high and low Km enzymes. J Biol Chem 1996;271:390–394

46. Wicksteed B, Brissova M, Yan W, et al. Conditional gene targeting in mouse pancreatic ß-Cells: analysis of ectopic Cre transgene expression in the brain. Diabetes 2010;59:3090–3098